Human Molecular Genetics, 1999, Vol. 8, No. 6 **1091–1098**

Defective intracellular transport of CLN3 is the molecular basis of Batten disease (JNCL)

Irma Järvelä+, Maarit Lehtovirta, Ritva Tikkanen[1], Aija Kyttälä and Anu Jalanko

National Public Health Institute, Laboratory of Human Molecular Genetics, Mannerheimintie 166, 00300 Helsinki, Finland and [1]Institute for Cell Biology, University of Bonn, Ulrich Haberland Strasse 61a, D-53121 Bonn, Germany

Received January 21, 1999; Revised and Accepted March 2, 1999

Batten disease [juvenile-onset neuronal ceroid lipofuscinosis (JNCL)], the most common progressive encephalopathy of childhood, is caused by mutations in a novel lysosomal membrane protein (CLN3) with unknown function. In this study, we have confirmed the lysosomal localization of the CLN3 protein by immunoelectron microscopy by co-localizing it with soluble and membrane-associated lysosomal proteins. We have analysed the intracellular processing and localization of two mutants, 461–677del, which is present in 85% of CLN3 alleles and causes the classical JNCL, and Q295K, which is a rare missense mutation associated with an atypical form of JNCL. Pulse–chase labelling and immunoprecipitation of the two mutant proteins in COS-1-cells indicated that 461–677del is synthesized as an ~24 kDa truncated polypeptide, whereas the maturation of Q295K resembles that of the wild-type CLN3 polypeptide. Transient expression of the two mutants in BHK cells showed that 461–677del is retained in the endoplasmic reticulum, whereas Q295K was capable of reaching the lysosomal compartment. The CLN3 polypeptides were expressed further in mouse primary neurons where the wild-type CLN3 protein was localized both in the cell soma and in neuronal extensions, whereas the 461–677del mutant was arrested in the cell soma. Interestingly, co-localization of the wild-type CLN3 and Q295K proteins with a synaptic vesicle marker indicates that the CLN3 protein might participate in synaptic vesicle transport/transmission. The data presented here provide clear evidence for a cellular distinction between classical and atypical forms of Batten disease both in neural and non-neural cells.

INTRODUCTION

Batten disease [juvenile-onset neuronal ceroid lipofuscinosis (JNCL)] is an autosomal recessive progressive encephalopathy that is characterized clinically by visual failure, epilepsy, psychomotor deterioration and premature death (1). Based on genetic and molecular analysis, a novel gene, *CLN3*, underlying Batten disease was identified (2). The predicted amino acid sequence of the CLN3 protein shows no homology with any known protein, but the computer-based structural analysis indicates several hydrophobic regions, suggesting that CLN3 represents an integral transmembrane protein (2–4). The high evolutionary conservation demonstrated with homologous genes in *Saccharomyces cerevisiae* (*YHC3*, Z49334), *Caenorhabditis elegans* (Z77656), mouse (U47106) and dog (L76281) suggests an important role for this protein in eukaryotic cells.

Since the cloning of the *CLN3* gene, 24 different mutations have been described in Batten disease (2,5–6). The most common mutation, 461–677del originating from the 1.02 kb deletion at the genomic level, removes 217 bp (exons 7 and 8) from the CLN3-coding region and is present in 85% of affected chromosomes. Our previous studies on phenotype–genotype correlation in Batten disease have shown that homozygosity for the 1.02 kb deletion is always associated with visual failure, psychomotor deterioration and early brain atrophy (7). However, a few Batten patients have been shown to carry an atypical phenotype where visual failure predominates but intellectual skills are preserved and a longer life span expected (5–6,8).

The biochemical function of the CLN3 protein has not yet been established. We have shown recently that the wild-type CLN3 protein is an ~43 kDa glycoprotein that co-localizes with lamp1 in the lysosomal compartment in transfected HeLa cells (9). Unlike soluble lysosomal enzymes, the CLN3 polypeptide is not secreted, supporting computer predictions which indicate that CLN3 is an integral membrane protein (9). Studies with yeast *S.cervisiae* have shown that the Batten homologue in yeast is localized to the yeast vacuole, an equivalent of the mammalian lysosome (10–12).

In this study, we have used immunoelectron microscopy to confirm the lysosomal localization of the wild-type CLN3-protein in a stably transfected NRK cell line using two different lysosomal markers, limpII and cathepsin D. The initial step in understanding the structure–function relationships in CLN3 involved the characterization of the intracellular trafficking of the two natural mutants of the protein that reveals important functional aspects of CLN3. These were the major 461–677del associated with the classical, severe form of JNCL and a missense mutation Q295K associated with an atypical, milder form of JNCL. The results indicated that, in both neural and non-neural cells, the intracellular transport of the deletion

+To whom correspondence should be addressed. Tel: +358 9 4744 8555; Fax: +358 9 4744 8480; Email: irma.jarvela@ktl.fi

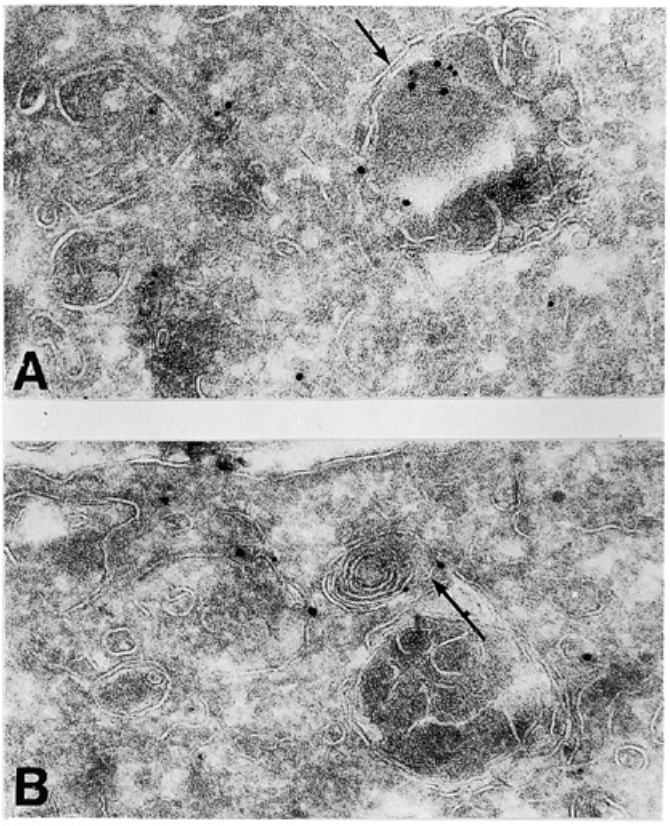

Figure 1. NRK cells stably transfected with the wild-type CLN3 construct were processed for cryoimmunoelectron microscopy and double labelled for 345/CLN3 polyclonal antibody (15 nm gold) and (**A**) cathepsin D (10 nm) or (**B**) limpII (10 nm). Lysosomal membranes are marked by an arrow in both panels.

mutant is severly hampered, whereas the Q295K polypeptide is capable of reaching lysosomes.

RESULTS

Immunoelectron microscopy

Several reports have suggested that CLN3 would actually be a mitochondrial protein largely due to the fact that the main accumulation product in Batten disease is the subunit c of the mitochondrial ATPase (13–15). Our previous data using immunofluorescence have provided evidence for the lysosomal localization of the CLN3 protein and for the lack of labelling in mitochondria (9), but a conclusive ultrastructural localization has not been performed so far. Therefore, we produced a recombinant normal rat kidney (NRK) cell line stably expressing CLN3 in order to study the localization of the CLN3 protein by means of cryoimmunoelectron microscopy. Ultrathin cryosections from the CLN3-NRK cells were double labelled for 345/CLN3 protein and two lysosomal proteins; limpII, an integral membrane protein, and a soluble lysosomal hydrolase cathepsin D. CLN3 was found to co-localize with both marker proteins in multivesicular/multilaminar structures that can be judged morphologically as late endosomes/lysosomes (Fig. 1). In addition to these structures, CLN3 was also detected at the Golgi/*trans*-Golgi network (TGN) and in more peripheral transport vesicles. Some particles were also detected at the plasma membrane (data not shown). However, the bulk of the label was found in late endosomes/lysosomes, demonstrating that CLN3 enters the endosomal/lysosomal compartment.

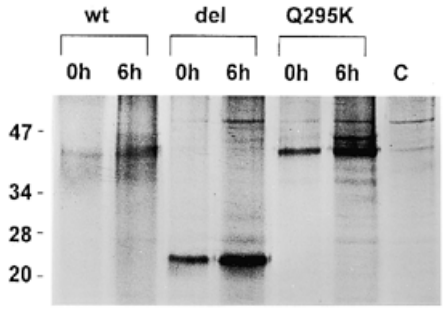

Figure 2. Pulse–chase analysis of the wild-type CLN3, 461–677del and Q295K polypeptides expressed in COS-1 cells. Cells were transiently transfected with the wild-type CLN3, 461–677del and Q295K constructs, immunoprecipitated by the 365/CLN3 antibody, pulse-labelled with [^{35}S]cysteine (Amersham) for 1 h and chased for 0 and 6 h, electrophoresed on an 11% SDS–polyacrylamide gel and visualized by fluorography. C, untransfected COS-1 cells (0 h) as a control.

Intracellular synthesis and processing of 461–677del and Q295K polypeptides

Our previous experiments on the intracellular processing and maturation of the wild-type CLN3 protein showed that it is an intracellular polypeptide of ~43 kDa that undergoes heterogeneous glycosylation (9). Here we have analysed the intracellular synthesis of two mutant polypeptides, 461–677del and Q295K. Mutagenesis of CLN3 cDNA was carried out *in vitro* and the mutant cDNA constructs were inserted into the pCMV5 expression vector. After transient transfection of COS-1 cells, the metabolically labelled polypeptides were immunoprecipitated using polyclonal peptide antibody 365/CLN3 which was generated against a peptide of amino acids 4–19 of CLN3. Figure 2 shows pulse–chase labelling and immunoprecipitation in COS-1 cells transfected with the wild-type CLN3, 461–677del and Q295K in pCMV5 vectors, labelled for 1 h and chased for 0 and 6 h. The wild-type CLN3 and Q295K proteins produced a similar polypeptide of ~43 kDa in size. The mutant construct 461–677del corresponding to the natural 217 bp deletion produced a truncated, ~24 kDa polypeptide (Fig. 2). The Q295K polypeptide was matured into two polypeptides resembling the differentially glycosylated wild-type CLN3 (9). No processing is observed with the 461–677del polypeptide (Fig. 2). Both peptide antibodies 365/CLN3 and 385/CLN3, designed from the 5' end (amino acids 4–19) and from the middle part of the CLN3 polypeptide (amino acids 242–258), respectively, detect bands of the same size in the immunoprecipitation of the wild-type CLN3 polypeptide (Fig. 2 and ref. 9).

Subcellular distribution of 461–677del and Q295K mutants in transfected BHK cells

We used the Fugene transfection method (Boehringer Mannheim, Mannheim, Germany) in baby hamster kidney (BHK)

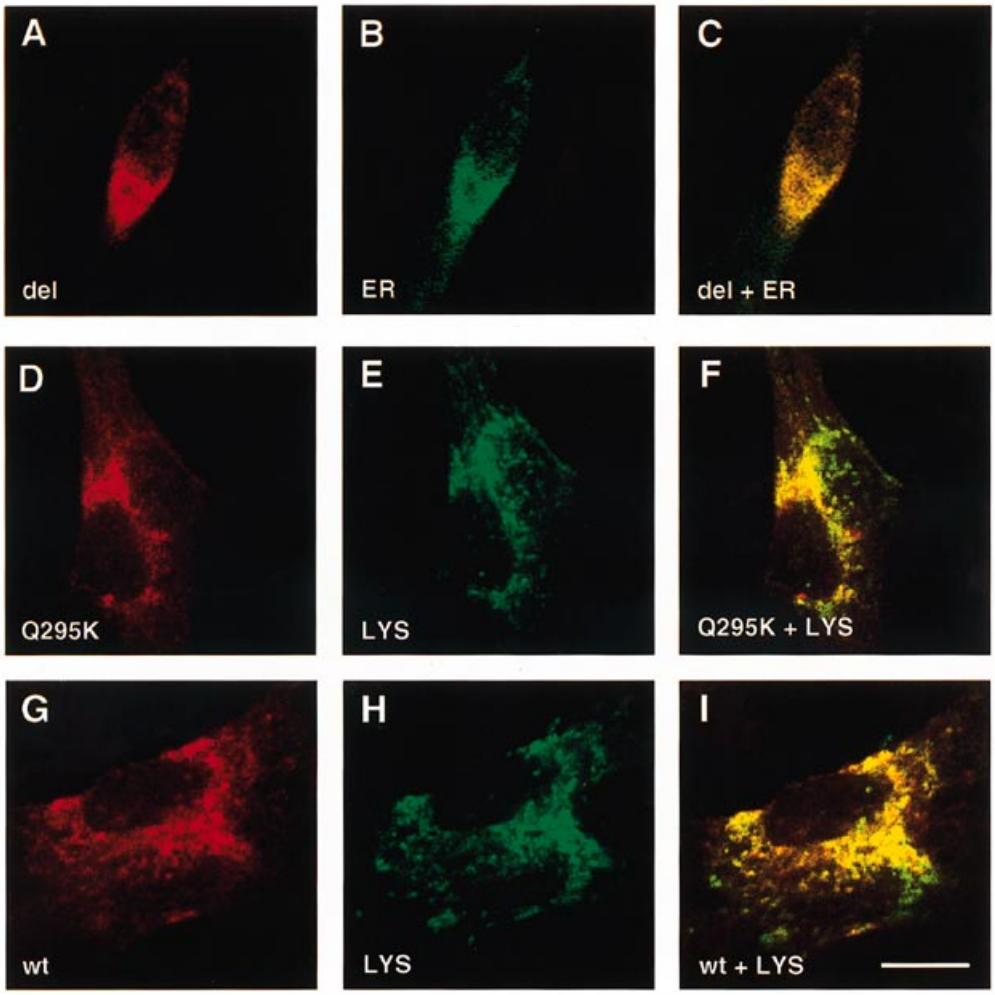

Figure 3. Distribution of 461–677del, Q295K and the wild-type CLN3 protein in Fugene-transfected BHK cells. Double immunofluorescence stainings of 461–677del and ER (**A**–**C**), Q295K (**D**–**F**) and the wild-type CLN3 protein and lysosomes (**G**–**I**) were carried out with polyclonal 365/CLN3 antibody for CLN3 protein, PDI for the ER, and monoclonal lgp120/4a1 antibody for the lysosomes/late endosomes. In colour overlays, the staining pattern of CLN3 (red) and subcellular compartmental markers (green) is shown (overlapping distribution in yellow). Bar = 10 μM.

cells to analyse the subcellular localization of the 461–677del and the Q295K missense mutant CLN3 polypeptides. Confocal microscopy was utilized to visualize the transfected cells after immunofluorescence staining with affinity-purified 365/CLN3 polyclonal antibody and markers for intracellular compartments. The 461–677del polypeptide was distributed throughout the cytoplasm as a reticular tubular network resembling the staining pattern for endoplasmic reticulum (ER) proteins. Double staining for the deletion protein and ER proteins using 365/CLN3 and protein disulfide isomerase (PDI) revealed a significantly overlapping staining pattern (Fig. 3). Retention of the 461–677del in the ER is in agreement with the finding that this protein was severely truncated in the pulse–chase analysis (Fig. 2).

The immunofluorescence staining pattern of the Q295K in transfected BHK cells closely resembled that of the wild-type CLN3 protein. The major finding is a punctate vesicular staining pattern typical of lysosomes. This was demonstrated further by double staining of the Q295K protein and lysosomes using the 365/CLN3 antibody and lgp120/4a1 which showed a clear co-distribution (Fig. 3). When compared with the wild-type CLN3 protein, however, the apparent number of vesicles in BHK cells infected with Q295K was smaller. The staining pattern of the wild-type CLN3 protein in Fugene-transfected BHK cells using the 365/CLN3 antibody was identical to the staining pattern in transfected HeLa cells using the 385/CLN3 antibody (Fig. 3 and ref. 9).

Subcellular distribution of the wild-type CLN3, 461–677del and Q295K mutants in mouse telencephalic primary neurons

Although ceroid and lipofuscin-like lipopigments accumulate in neural and non-neural tissues of Batten patients, the symptoms manifest only in the central nervous system (16). Therefore, the question arises of whether a neuron-specific mechanism exists for the processing and transport of the CLN3 protein. In an attempt to answer those questions, immunofluorescence studies were carried out to localize the wild-type CLN3 in murine primary telencephalic neurons. Due to its high

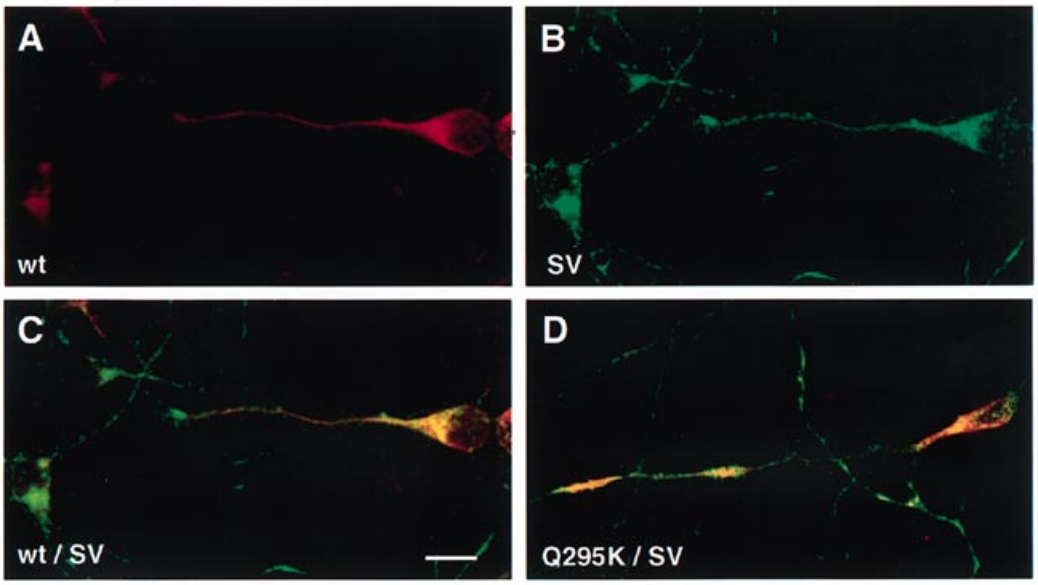

Figure 4. Distribution of the wild-type CLN3 protein and Q295K in SFV-infected mouse primary telencephalic neurons. Double immunofluorescence stainings of the wild-type CLN3 (**A** and **C**) (red) and Q295K (**D**) (red), and synaptic vesicles (**B**) (green) was carried out with the 385/CLN3 antibody for the CLN3 protein and with synaptic vesicle antibody (SV2) with confocal microscopy. Overlapping distribution is shown in yellow. Bar = 10 μM.

expression capacity and efficient infection of neurons, recombinant Semliki forest virus (SFV) vector (17) was used as a transport vehicle. Neuron-specific expression of the wild-type CLN3 was detected by double labelling the neurons with a monoclonal antibody SV2 for mouse synaptic vesicles and 385/CLN3 antibody. The wild-type CLN3 distributed along neural processes towards the synaptic ends and growth cones, and co-localized with a synaptic vesicle protein, SV2 (Fig. 4). CLN3 was distributed throughout the primary neurons and showed clear co-localization with a lysosomal marker rat monoclonal lamp1 (Fig. 5).

The telencephalic cell cultures were also infected with the two mutant CLN3 proteins, 461–677del and Q295K. The 461–677del protein was detected only in the cell soma of mouse primary neurons, revealing a more diffuse staining pattern that co-localized with PDI (Fig. 4). Immunoreactivity of 461–677del was also absent from the neural extensions, indicating a defect in the intracellular trafficking of the deletion mutant (Fig. 5). In contrast, the immunofluorescence staining pattern of the Q295K protein in mouse primary neurons closely resembled that of the wild-type protein. The Q295K protein was detected in neuronal extensions using double stainings with 385/CLN3 and antibody for synaptic vesicle protein, SV2, reflecting the ability of this mutant to move along the axon towards the neural plate (Fig. 4).

DISCUSSION

In the search for functionally important domains in the CLN3 protein defective in Batten disease, the most common cause of dementia in childhood, we describe here the intracellular processing and expression of two CLN3 mutants, the major 461–677del, responsible for the classical JNCL, and a missense mutation Q295K in exon 11, responsible for the atypical JNCL in neuronal and non-neuronal cells. We also confirm the lysosomal localization of the CLN3 protein in transfected NRK cells by immunoelectron microscopy.

The immunoelectron microscopic data presented here confirm our previous findings that the CLN3 protein is transported to the lysosomes (9). The majority of the labelled wild-type CLN3 protein was detected in multivesicular/multilaminar structures that can be judged morphologically as late endosomes/lysosomes. Localization of CLN3 at the Golgi/TGN and in more peripheral transport vesicles reflects its intracellular trafficking through the ER–Golgi compartments. Interestingly, some particles could be demonstrated also at the plasma membrane, suggesting that the CLN3 protein may recycle through the plasma membrane on its way to the lysosomes. These findings are in agreement with the immunofluorescence studies of the wild-type CLN3 protein in HeLa cells where, in addition to clear co-localization with the lysosomal membrane protein lamp1, some small vesicles remained unstained (9). Some lysosomal membrane proteins reach lysosomes indirectly via the cell surface and endocytosis, others exit the TGN in clathrin-coated vesicles and are delivered more directly via endosomes to lysosomes without appearing at the plasma membrane (18–22). Questions concerning the detailed intracellular trafficking route of the CLN3 protein have to be addressed in a separate study.

Previous studies have shown that variability in the severity of Batten disease is due in part to specific mutations in the *CLN3* gene (2,5–8). To understand how mutations in *CLN3* disrupt the function of the CLN3 protein and to learn more about the relationship between genotype and phenotype, we studied two natural CLN3 mutants, the 461–677del and a rare missense mutation Q295K on exon 11, which originates from a nucleotide substitution of G1020 to A resulting in an amino acid change of glutamine to lysine (5,6,8). The 461–677del in a homozygous form always causes a severe phenotype includ-

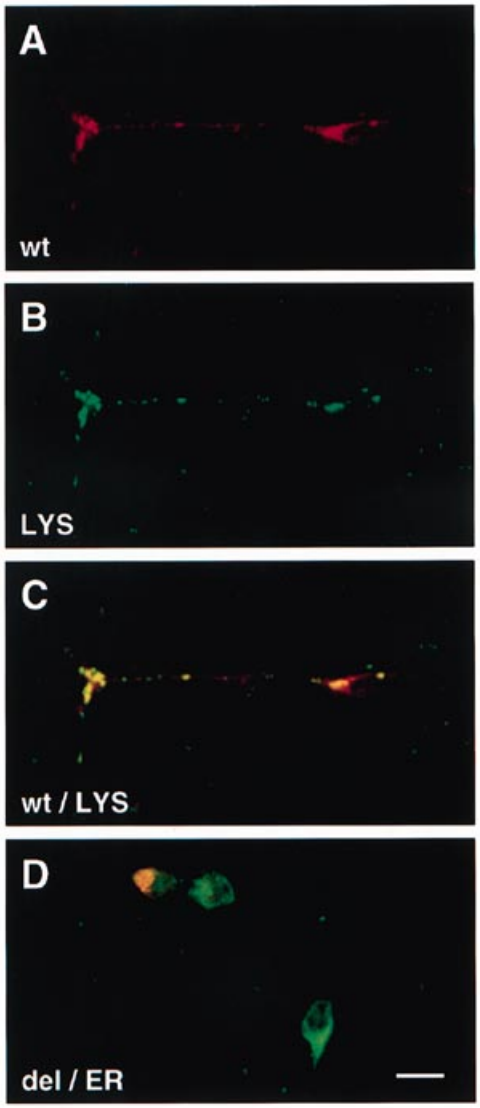

Figure 5. Double immunofluorescence stainings of the wild-type CLN3 protein (**A** and **C**) with the 385/CLN3 antibody (red) and lamp1 (**B** and **C**) (green) for lysosomes with confocal microscopy. The 461–677del protein stained with the 365/CLN3 (red) and PDI for ER (green) in SFV-infected mouse primary telencephalic neurons. (**D**) Overlapping distribution is shown in yellow (C and D). Bar = 10 μM.

ing blindness, epilepsy, dementia and early death at ~24 years of age (5,7). When this mutant was transiently expressed in BHK cells, no punctate vesicles were detected. Instead, a clear co-localization with the ER marker, PDI, was shown. We propose that the truncated ~24 kDa polypeptide resulting from 461–677del is severely misfolded, which prevents its targeting from the ER. Since only about one-third of the original CLN3 polypeptide is left, it is highly probable that both functionally important domains and lysosomal targeting signals, typically located at the C-terminal end of lysosomal membrane proteins (18–22), are lost in the 461–677del polypeptide. The ER retention data obtained with the 461–677del mutant indicate that the important areas for CLN3 function lie in the Golgi–endosome–lysosome route.

Q295K has been described in two American siblings of German origin (8) and in one Finnish patient (5,6). This 'mild' phenotype of JNCL is characterized by predominantly ocular symptoms and a longer life span. However, the age of onset and severity of visual failure are similar in both classical and atypical phenotypes (7,8). The greatest difference is found in the severity of the brain damage; the first signal intensity changes can be found in the severe phenotype at ~10 years of age (7), whereas in the mild phenotype magnetic resonance imaging (MRI) has been normal even at the age of 39 years (8). Q295K has been predicted to lie in the fourth transmembrane domain of the CLN3 protein (5). Expression of Q295K in BHK cells showed that this mutant is capable of reaching its final destination in lysosomes. The amino acid change, uncharged polar amino acid glutamine to positively charged hydrophilic amino acid lysine, might change the conformation of one of the transmembrane domains of the CLN3 protein. It remains to be seen whether this causes delayed trafficking and/or inefficient function of the CLN3 protein. A similar effect might underlie another Batten mutation, L101P, which also causes a mild phenotype and has been predicted to lie in the first transmembrane domain (5). In JNCL, the retina is affected by accumulation of disease-specific lipopigments in neuronal perikarya and retinal pigment epithelial (RPE) cells (23), clinically detectable as a 'salt and pepper retinopathy' (1). The RPE is known to possess an extremely active lysosomal system (24). It is therefore conceivable that already mildly disturbed lysosomal membrane function and turnover will be harmful for the retinal function, which might explain why the retina is the first cell type affected in JNCL.

Accumulation of ceroid and lipofuscin-like lipopigments in neural and non-neural tissues of patients is the hallmark of JNCL and all other NCLs (16). However, the symptoms reflect the disease only in the central nervous system. Therefore, the question arises of whether a neuron-specific mechanism could be the primary cause for this group of diseases. We addressed this question by analysing the subcellular localization of the wild-type CLN3 and the two mutants in SFV-infected mouse primary telencephalic neurons. Co-localization of the wild-type CLN3 protein with lysosomal lamp1 in cultured telencephalic neurons is in agreement with its localization in non-neuronal cells (9) and in stable transfected NRK cells using two other lysosomal markers, limpII and cathepsin D. In neural infections, 461–677del was retained in the cell soma, closely resembling the staining pattern of AGU_{Fin}, a mutated lysosomal aspartylglucosaminidase polypeptide which has been localized to the ER in both non-neural and neural cells (25–27). No difference was detected in the distribution of the 461–677del mutant in neural and non-neural cells. The distribution of the Q295K mutant in mouse primary neurons closely resembles that of the wild-type CLN3.

Co-localization of the CLN3 protein with the synaptic vesicle marker SV2 raises the possibility that the CLN3 protein has some function in neuronal endo- or exocytosis. This is supported further by the fact that the CLN3 protein has been shown to be phosphorylated by serine/threonine kinases (28), and phosphorylation might affect the exocytic process (for reviews, see refs 29–31). The synaptic end of a neuron is loaded with vesicles, and co-localization of the CLN3 protein with the SV2 marker is only indicative of its localization in synaptic vesicles. The donor compartment for synaptic

vesicles has been proposed to be transferrin receptor-containing early endosomes (32), which would explain the simultaneous localization of CLN3 in the endosomal–lysosomal pathway and in synaptic vesicles. The fact that palmitoyl protein thioesterase, the protein defective in the infantile form of NCL, has also recently been localized to the neuronal synapses (O. Heinonen, A. Kyttälä, E. Lelmus, T. Pauries, L. Peltonen and A. Jalenko, manuscript submitted for publication) makes this hypothesis even more intriguing and focuses the functional studies of NCL proteins on synaptic transmission.

MATERIALS AND METHODS

In vitro mutagenesis

Mutagenesis was performed with the Chameleon double-stranded, site-directed mutagenesis kit (Stratagene) as suggested by the manufacturer. Mutants are named according to the amino acids deleted or their single letter amino acid code (5). For the template, we used the full-length coding region of *CLN3* cDNA cloned into the *Eco*RI–*Bam*HI site of the pGEM4Z expression vector. For restriction enzyme selection, we used oligonucleotides that are located in the polylinker region of pGEM4Z. The 217 bp deletion was mutagenized in two phases, by first removing nucleotides 461–561 using removal of the *Sal*I site and, from the resulting mutant, nucleotides 562–677 were deleted using *Sph*I removal in the selection primer of the pGEM4Z cloning vector. The missense mutation Q295K was mutagenized by *Sal*I removal only. The mutations of the mutagenized clones were confirmed by sequencing (33). The mutagenized clones were excised and inserted into the *Eco*RI–*Bam*HI cloning site of pCMV5 (34) and SFV expression vectors (17) for expression studies.

Cell culture and transfection

BHK cells were cultured in Glasgow minimal essential medium (MEM) supplemented with 5% fetal calf serum (FCS), 2 mM L-glutamine, 10% tryptose phosphate broth, 20 mM HEPES pH 7.0, 100 IU/ml penicillin and 100 g/ml streptomycin. The cells were transfected with 1 mg of the wild-type CLN3 and mutant constructs using the Fugene-transfection method (Boehringer Mannheim) as suggested by the manufacturer.

Timed-pregnant mice (C57BL) were anaesthetized with carbon dioxide and killed. Embryos of 14–15 days post-fertilization (E14–15) were removed from the uterus and placed in ice-cold 0.1 M phosphate-buffered saline (PBS) without Ca^{2+} and Mg^{2+}, pH 7.2–7.4, supplemented with 20 mM glucose. Telencephalic structures were cleared from blood vessels and meninges. Individual cells were isolated by cutting the tissue into small cubes, triturated in PBS, and incubated in trypsin–EDTA (0.1%/0.4 mM) supplemented with DNase I (10 µg/ml) for 15 min at 37°C. Trypsin was inactivated by 10% FCS and cells were centrifuged for 2–3 min at 1000 r.p.m. The supernatant was discarded and the pellet was resuspended in Neurobasal medium (Gibco BRL Life Technologies, Gaithersburg, MD) supplemented with antibiotics, 0.5 mM L-glutamine, 2.5 µM glutamic acid and 2% B-27 (Gibco BRL). Neurons were plated on poly-D-lysine hydrobromide-coated (50 µg/ml; Sigma, Steinheim, Germany) cell culture dishes and cultured at 37°C under 5% CO_2.

Metabolic labelling experiments

COS-1 cells were maintained in Dulbecco's modified Eagle's medium (DMEM) supplemented with 10% FCS and antibiotics. For transfection, the cells were seeded at a density of 400 000 cells per well on a 6-well plate and grown overnight. Transfection was performed with 5 mg of the plasmid construct using the DEAE–dextran/chlorokine method (35). The cells were incubated for 4 h with a mixture of DNA and DEAE–dextran (100 µg/ml) in 1.5 ml of serum-free DMEM. This mixture was replaced with 100 µg/ml chlorokine in serum-free DMEM, incubated for 3 h and refreshed with serum-containing DMEM. The medium was refreshed daily and the cells were pulse-labelled with 100 mg/ml of [^{35}S]cysteine (3000 Ci/mmol; Amersham, Little Chalfont, UK) in cysteine-free medium on the third day after transfection. After a 1 h pulse, and a chase time of 6 h in DMEM without FCS, the cells were harvested by trypsinization and lysed by freeze–thawing in 100 ml of 1% Triton X-100 in PBS. The cells were immunoprecipitated by polyclonal 365/CLN3 antibody and formalin-fixed *Staphylococcus aureus* cells (Immuno-Precipitin; Gibco BRL), according to Proia *et al.* (36). The immunoprecipitated polypeptides were separated on an 11% SDS–polyacrylamide gel (37) and visualized by fluorography using Amplify reagent (Amersham).

Generation of stably transfected cell lines

NRK cells were transfected with 4 µg of the wild-type *CLN3* cDNA construct in pCMV5 vector by lipofection using the Lipofectin reagent (Gibco BRL). For selection of the stably transfected clones, the pCIneo plasmid (Promega, Leiden, The Netherlands) carrying a neomycin selection marker was co-transfected and the clones were selected with 500 µg/ml geneticin sulfate starting 2 days after transfection. Positive clones were screened by immunofluorescence using the 345/CLN3 polyclonal antibody to verify their homogeneity.

Preparation of the recombinant SFVs and infections

The pSFV-wt-CLN3, pSFV-Q295K, pSFV-461–677del and the pSFV-helper 1 were linearized with *Spe*I, and run-off transcription with the SP6 RNA polymerase (Pharmacia, Milwaukee, WI) was performed in a volume of 50 µl (18). BHK cells (5×10^6 cells per electroporation) were trypsinized gently with trypsin–EDTA, washed once with complete BHK medium and twice with ice-cold electroporation buffer (0.27 mM KCl, 1.47 mM KH_2PO_4, 137 mM NaCl, 8.06 mM $Na_2HPO_4 \cdot 7H_2O$, pH 7.2), and resuspended in 0.85 ml of the same buffer. The pSFV vectors and pSFV-helper transcription mixes (20 µl of each per electroporation) were added to the cells and the mixture was transferred quickly into a Bio-Rad Gene-Pulser cuvette (0.4 cm electrode gap). After two pulses (Bio-Rad Gene Pulser, 0.85kV, 25 µF), the cells were diluted in 16 ml of complete BHK medium and incubated for 36 h. The culture supernatant was collected and cleared by low-speed centrifugation. The supernatant was frozen in 500 µl aliquots at –70°C. The virus-containing supernatant was titrated on BHK cells as described by Olkkonen *et al*. (17). Infections were per-

formed by diluting the recombinant SFV in serum-free medium. Telencephalic neurons had been maintained in culture for 7–14 days, infection was continued for 1 h at 37°C/5% CO_2, then the virus solution was drained and the incubation was continued for 6–10 h.

Antibodies

The polyclonal rabbit antibodies, 345/CLN3 and 365/CLN3, directed against a synthetic peptide corresponding to amino acid residues 4–19, and a polyclonal rabbit antibody 385/CLN3, directed against a synthetic peptide corresponding to amino acid residues 242–258 of the full-length CLN3 cDNA, were prepared as described by Järvelä *et al*. (9). For double immunostaining, 365/CLN3 or 385/CLN3 antibody (1:150) was combined with anti-synaptic vesicles (SV2), developed by Kathleen M. Buckley (Harvard Medical School, Boston, MA), or rat anti-LAMP-1 (ID4B), developed by Thomas August (Johns Hopkins University, Baltimore, MD), which were obtained from the Developmental Studies Hybridoma Bank developed under the auspices of the NICHD and maintained by the University of Iowa (Iowa City, IA). Anti-PDI (1:200; StressGen Biotechnologies, Victoria, Canada) was used to detect the ER, and lgp120/4a1 (38) to detect the lysosomes. The secondary antibodies used in immunofluorescence microscopy were tetramethylrhodamine isothiocyanate (TRITC)-conjugated goat anti-rabbit IgG (1:150) and fluorescein isothiocyanate (FITC)-conjugated goat anti-mouse or goat anti-rat IgG (1:150) (Immunotech, Marseille, France).

Immunofluorescence and immunoelectron microscopy

Both BHK cells and neurons were fixed with 4% paraformaldehyde in PBS for 15 min at room temperature, permeabilized with 0.2% saponin (Sigma) (BHK cells) and 0.05% Triton X-100 (Sigma) (neurons) for 15 min. For 365/CLN3 antibody, we also used 6 M guanidine hydrochloride in PBS for 10 min to denature the antigen. Unspecific binding was blocked with 0.5% bovine serum albumin (BSA; Sigma) in PBS for 15 min. Primary antibodies (1:150) were incubated in blocking buffer for 1 h at room temperature. The secondary antibody incubation was performed with TRITC-conjugated goat anti-rabbit IgG, or with FITC-conjugated goat anti-mouse or anti-rat IgG (1:150; Immunotech) in blocking buffer for 40 min. The coverslips were mounted in GelMount (Biomeda, Foster City, CA) and viewed with a Leica confocal microscope. Immunoelectron microscopy was performed according to the method of Tokuyasu (39). Stably transfected NRK cells were fixed with 2% paraformaldehyde and 0.2% glutaraldehyde in 0.1 M K-phosphate buffer (PB) for 30 min at room temperature and then for a further 1.5 h on ice after exchange of the fixative. The cells were embedded in 10% gelatin, immersed in 2.3 M sucrose in 0.2 M PB overnight in the cold room, with continuous mixing, and mounted for cryosectioning. Ultrathin cryosections were cut and double labelled (40) for 345/CLN3 and either limpII or cathepsin D. The primary antibodies were detected with protein A conjugated with 10 or 15 nm gold (PAG, purchased from the Laboratory of Cell Biology, University of Utrecht). Cathepsin D was detected with a polyclonal rabbit serum KII-S7 (41) and limpII with a polyclonal antiserum against rat limpII (42). Immunolabelled sections were contrasted with uranyl acetate, embedded into uranyl-methyl cellulose and viewed with a Philips CM 120 electron microscope with a voltage of 80 kV.

ACKNOWLEDGEMENTS

We thank Auli Haikka for excellent technical assistance and Vesa M. Olkkonen for many helpful discussions. We are grateful to Jean Gruenberg (Geneva, Swizerland) for lgp120/4a1 antibody. This work was supported by the Sigrid Juselius Foundation, the Finnish Cultural Foundation and the Foundation for Pediatric Research (Ulla Hjelt Fond).

REFERENCES

1. Santavuori, P. (1988) Review: neuronal ceroid lipofuscinoses in childhood. *Brain Dev.*, **10**, 80–83.
2. The International Batten Disease Consortium (1995) Isolation of a novel gene underlying Batten disease (CLN3). *Cell*, **82**, 949–957.
3. Mitchison, H.M., Munroe, P.B., O'Rawe A.M., Taschner, P.E.M., de Vos N., Kremmioditis, G., Lensink, I., Munk, A.C., D'Arigo K.L., Anderson, J.W., Lerner, T.J., Moyzis, R.K., Callen, D.F., Breuning, M.H., Doggett, N.A., Gardiner, R.M. and Mole, S.E. (1997) Genomic structure and complete nucleotide sequence of the Batten disease gene, *CLN3*. *Genomics*, **40**, 346–350.
4. Janes, R.W., Munroe, P.B., Mitchison, H.M., Gardiner, R.M., Mole, S.E. and Wallace, B.A. (1996) A model for Batten disease protein CLN3: functional implications from homology and mutations. *FEBS Lett.*, **399**, 75–77.
5. Munroe, P.B., Mitchison, H.M., O'Rawe, A.M., Anderson, J.W., Boustany, R.M., Lerner, T.J., Taschner, P.E.M., deVos, N., Breuning, M.H., Gardiner, R.M. and Mole, S.E. (1997) Spectrum of mutations in the Batten disease gene (*CLN3*). *Am. J. Hum. Genet.*, **61**, 310–316.
6. Lauronen, L., Munroe, P.B., Järvelä, I., Autti, T., Mitchison, H.M., O'Rawe, A.M., Gardiner, R.M., Mole, S.E., Puranen, J., Häkkinen, A.-M., Kirveskari, E. and Santavuori, P. (1999) Delayed classical and protracted phenotype of compound heterozygous juvenile NCL. *Neurology*, **52**, 360–365.
7. Järvelä, I., Autti, T., Lamminranta, S., Åberg, L., Raininko, R. and Santavuori, P. (1997) Clinical and MRI-findings in Batten disease—analysis of the major mutation (1.02 kb deletion). *Ann. Neurol.*, **42**, 799–802.
8. Wisniewski, K.E., Zhong, N., Kaczmarski, W., Kaczmarski, A., Kida, E., Brown, W.T., Schwarz, K.O., Lazzarini, A.M., Rubin, A.J., Stenroos, E.S., Johnson, W.G. and Wisniewski, T.M. (1998) Compound heterozygous genotype is associated with protracted juvenile neuronal ceroid lipofuscinosis. *Ann. Neurol.*, **43**, 106–110.
9. Järvelä, I., Sainio, M., Rantamäki, T., Olkkonen, V.M., Carpen, O., Peltonen, L. and Jalanko, A. (1998) Biosynthesis and intracellular targeting of the CLN3 protein defective in Batten disease. *Hum. Mol. Genet.*, **7**, 85–90.
10. Pearce, D.A. and Sherman, F. (1997) *BTN1*, a yeast gene corresponding to the human gene responsible for Battens-disease, is not essential for viability, mitochondrial function, or degradation of mitochondrial ATP synthase. *Yeast*, **13**, 691–697.
11. Pearce, D.A. and Sherman, F. (1998) A yeast model for the study of Batten disease. *Proc. Natl Acad. Sci. USA*, **95**, 6915–6918.
12. Croopnick, J.B., Choi, H.C. and Mueller, D.M. (1998) The subcellular location of the yeast *Saccharomyces cerevisiae* homologue of the protein defective in the juvenile form of Batten disease. *Biochem. Biophys. Res. Commun.*, **250**, 335–341.
13. Fearnley, I.M., Walker, J.E., Martinus, R.D., Jolly, R.D., Kirkland, K.B., Shaw, J. and Palmer, D.N. (1990) The sequence of the major protein stored in ovine ceroid lipofuscinosis is identical with that of the dicyclohexylcarbodi-imide-reactive proteolipid of mitochondrial ATP synthase. *Biochem. J.*, **268**, 751–758.
14. Palmer, D.N., Fearnley, I.M., Walker, J.E., Hall, N.A., Lake, B.D., Wolfe, L.S., Haltia, M., Martinus, R.D. and Jolly, R. (1992) Mitochondrial ATP-synthase subunit C storage in the ceroid lipofuscinosis (Batten disease). *Am. J. Med. Genet.*, **42**, 561–567.
15. Katz, M.L., Gao, C.-L., Prabhakaram, M., Shibuya, H., Liu, P.-C. and Johnson, G.S. (1997) Immunochemical localization of the Batten disease (CLN3) protein in retina. *Invest. Ophthalmol. Vis. Sci.*, **38**, 2375–2386.

16. Zeman, W. and Dyken, P. (1969) Neuronal ceroid lipofuscinosis (Batten's disease): relationship to amaurotic familial idiocy? *Pediatrics*, **44**, 570–583.
17. Olkkonen, V.M., Liljeström, P., Garoff, H., Simons, K. and Dotti, C.G. (1993) Expression of heterologous proteins in cultured rat hippocampal neurons using the Semliki forest virus vector. *J. Neurosci. Res.*, **35**, 445–451.
18. Williams, M.A. and Fukuda, M. (1990) Accumulation of membrane glycoproteins in lysosomes requires a tyrosine residue at a particular position in the cytoplasmic tail. *J. Cell Biol.*, **111**, 955–966.
19. Harter, C. and Mellman, I. (1992) Transport of the lysosomal membrane glycoprotein lgp120 (lgp-A) to lysosomes does not require appearance on the plasma membrane. *J. Cell Biol.*, **117**, 311–325.
20. Johnson, K.F. and Kornfeld, S. (1992) The cytoplasmic tail of the mannose 6-phosphate/insulin-like growth factor II receptor has two signals for lysosomal enzyme sorting in the Golgi. *J. Cell Biol.*, **119**, 249–257.
21. Johnson, K.F. and Kornfeld, S. (1992) A His–leu–leu sequence near the carboxyl terminus of the cytoplasmic domain of the cation-dependent mannose-6-phosphate receptor is necessary for the lysosomal enzyme sorting function. *J. Biol. Chem.*, **267**, 17110–17115.
22. Letourneur, F. and Klausner, R.D. (1992) A novel di-leucine motif and a tyrosine-based motif independently mediate lysosomal targeting and endocytosis of CD3 chains. *Cell*, **69**, 1143–1157.
23. Goebel, H.H., Köhneke, B., Koppang, N. and Armstrong, D. (1983) Ultrastructural studies on the retinal pigment epithelium in the neuronal ceroid lipofuscinoses. *Opthalmic Paediatr. Genet.*, **3**, 29–37.
24. Hohman, T.C. and Bowers, B. (1984) Hydrolase secretion is a consequence of membrane recycling. *J. Cell Biol.*, **98**, 246–252.
25. Ikonen, E., Baumann, M., Grön, K., Syvänen, A.-C., Enomaa, N., Halila, R., Aula, P. and Peltonen, L. (1991) Aspartylglucosaminuria: cDNA encoding human aspartyl-glucosaminidase and the missense mutation causing the disease. *EMBO J.*, **10**, 51–58.
26. Riikonen, A., Ikonen, E., Sormunen, R., Lehto, V.-P., Peltonen, L. and Jalanko, A. (1994) Dissection of molecular consequences of a double mutation causing a lysosomal disease. *DNA Cell Biol.*, **13**, 257–264.
27. Kyttälä, A., Heinonen, O., Peltonen, L. and Jalanko, A. (1998) Expression and endocytosis of lysosomal aspartylglucosaminidase in mouse primary neurons. *J. Neurosci.*, **18**, 7750–7756.
28. Michalewski, M.P., Kaczmarski, W., Golabek, A.A., Kida, E., Kaczmarski, A. and Wisniewski, K.E. (1998) Evidence for phosphorylation of CLN3 protein associated with Batten disease. *Biochem. Biophys. Res. Commun.*, **253**, 458–462.
29. Linial, M. (1997) SNARE proteins—why so many, why so few? *J. Neurochem.*, **69**, 1781–1798.
30. Ferro-Novick, S. and Jahn, R (1994) Vesicle fusion from yeast to man. *Nature*, **370**, 191–193.
31. Nixon, R.A. and Cataldo, A.M. (1995) The endosomal–lysosomal system of neurons: new roles. *Trends Neurosci.*, **18**, 489–496.
32. Cameron, P.L., Sudhof, T.C., Jahn, R. and De Camilli, P. (1991) Colocalization of synaptophysin with transferrin receptors: implications for synaptic vesicle biogenesis. *J. Cell Biol.*, **115**, 151–164.
33. Sanger, F., Nicklen, S. and Coulson, A.R. (1977) DNA-sequencing with chain termination inhibitors. *Proc. Natl Acad. Sci. USA*, **74**, 5463–5467.
34. Andersson, S., Davis, D.L., Dahlbäck, H., Jörnvall, H. and Russell, D.W. (1989) Cloning, structure and expression of the mitochondrial cytochrome P-450 sterol 26-hydroxylase, a bile acid biosynthetic enzyme. *J. Biol. Chem.*, **264**, 8222–8229.
35. Luthman, H. and Magnusson, G. (1983) High efficiency polyoma DNA transfection of choloroquine treated cells. *Proc. Natl Acad. Sci. USA*, **11**, 1295–1307.
36. Proia, R.L., d'Azzo, A. and Neufeld, E.F. (1984) Association of α- and β-subunits during the biosynthesis of β-hexosaminidase in cultured human fibroblasts. *J. Biol. Chem.*, **59**, 3350–3354.
37. Laemmli, U.K. (1970) Cleavage of structural proteins during the assembly of the head of bacteriophage T4. *Nature*, **227**, 680–685.
38. Aniento, F., Emans, N., Griffiths, G. and Gruenberg, J. (1993) Cytoplasmic dynein-dependent vesicular transport from early to late endosomes. *J. Cell Biol.*, **123**, 1373–1387.
39. Tokuyasu, K.T. (1986) Application of cryomicrotomy to immunocytochemistry. *J. Microsc.*, **143**, 139–149.
40. Slot, J.W., Geuze, H.J., Gigengack, S., Lienhard, G.E. and James, D. (1991) Immunolocalization of the insulin regulatable glucose transporter in brown adipose tissue of the rat. *J. Cell Biol.*, **113**, 123–135.
41. Pohlmann, R., Wendland, M., Boeker, C. and von Figura, K. (1995) The two mannose-6-phosphate receptors transport distinct but overlapping complements of lysosomal proteins. *J. Biol. Chem.*, **270**, 27311–27318.
42. Nakayama, Y., Hisano, T., Okimoto, T., Tanaka, Y., Ishikawa, T., Himeno, M., Ono, M. and Kuwano, M. (1994) *Cell Struct. Funct.*, **19**, 197–409.